

Numerical Simulation of the Mantle Convection and Subduction Process

Project Representative

Yoshio Fukao Institute for Research on Earth Evolution, Japan Agency for Marine-Earth Science and Technology

Authors

Yoshio Fukao ^{*1}, Tomoeeki Nakakuki ^{*2}, Masanori Kameyama ^{*3}, Takatoshi Yanagisawa ^{*1},
Yasuko Yamagishi ^{*1}, Yujiro Suzuki ^{*1}, Atsushi Suzuki ^{*4}, Motoyuki Kido ^{*5}, Masaki Ogawa ^{*6},
Takao Eguchi ^{*7}, Yasuyuki Iwase ^{*7}, Takashi Nakagawa ^{*8}, Michio Tagawa ^{*2},
Yoshito Hirayama ^{*7}, Millard F. Coffin ^{*9}, John Baumgardner ^{*10}, Mark Richards ^{*11},
Dave Stegman ^{*12} and Stephan Labrosse ^{*13}

*1 Institute for Research on Earth Evolution, Japan Agency for Marine-Earth Science and Technology

*2 Department of Earth and Planetary Systems Science, Hiroshima University

*3 The Earth Simulator Center, Japan Agency for Marine-Earth Science and Technology

*4 Department of Mathematical Science, Kyushu University

*5 Research Center for Prediction of Earthquakes and Volcanic Eruptions, Tohoku University

*6 Graduate School of Arts and Sciences, University of Tokyo

*7 Department of Earth and Ocean Sciences, National Defense Academy

*8 Department of Earth and Planetary Science, University of Tokyo

*9 Ocean Research Institute, University of Tokyo

*10 Theoretical Division, Los Alamos National Laboratory

*11 Department of Earth and Planetary Science, University of California, Berkeley

*12 School of Mathematical Sciences, Monash University

*13 Institut de Physique du Globe de Paris

The dynamics and evolution of the Earth's mantle are considered to be influenced by several complexities of the physical processes. In order to understand the mantle convection in the Earth, a numerical simulation is a very effective tool. On the other hand, the internal structure and the evolution of the mantle have been inferred by the geophysical and the geological observations. The seismic tomography reveals the large scale flow of the mantle convection, and it also illustrates some ancient slabs are stagnant in mantle transition zone. Our goal is to construct the models of mantle convection and caused volcanism which are consistent with these observational results. In this fiscal year, our main target is to make up models of "subduction" and "stagnant slab". We improved both global and regional codes for mantle convection, and made clear the conditions to generate stagnant structures. We also succeeded in simulating realistic volcanic eruption clouds.

Keywords: mantle convection, plate motion, subduction zone, stagnant slab, volcanic eruption

1. Introduction

The Earth's mantle is composed of silicate rocks, and on long time scales, it acts like a highly viscous fluid. The mantle also acts as a heat engine; it flows slowly in order to transport the heat from the hot interior to the cool surface. This convective flow in the mantle is observed as the motion of tectonic plates on the Earth's surface. The motion of surface plates in turn drives seismicity, volcanism and mountain building at the plate margins. Thus, the mantle convection is

the origin of the geological and geophysical phenomena observed at the Earth's surface.

Seismic tomography enables us to "see" the internal structure of the mantle. It illustrates the behavior of slabs, that is, ancient plates subducted in the mantle (review by Fukao et al.¹⁾). Some of the slabs stagnate in the mantle transition zone while the others penetrate into the lower mantle. Because the slab is an expression of downwelling flow in the mantle convection, the mechanisms to generate the various

styles of subducted slabs in the mantle transition zone are important to understand layering structure of the mantle convection. It is also very important for our life to understand the nature and behavior of "subduction" and "stagnant slab", because the Japanese Islands locate at the subduction zone, and slab stagnation are widely observed below the East Asia.

The aim of this project is to make up a comprehensive model of the dynamics and evolution of the Earth's mantle, and to simulate phenomena related with subduction. To this goal, we aim at developing numerical models which are consistent with the observations such as seismic tomography and geological evidence. The research of this project is divided in three subgroups, according to the nature of phenomena to be considered. First subgroup deals with 3-D global mantle flow in spherical shell geometry, and aims at understanding the large spatial scale dynamics and long-term evolution of the Earth (section 2 and 3 in this report). Second subgroup deals with 2-D regional mantle flow in rectangular geometry, and aims at modeling the stagnant structure of slabs consistent with seismic tomography and surface

plate motion (section 4). Third subgroup deals with the products of subduction processes emerged at the surface of the Earth, especially relating to volcanoes (section 5).

2. High Rayleigh number convection in a spherical shell

In this section, we discuss the convective pattern and the efficiency of the heat transport of the simple Rayleigh-Bénard convection model with Bousinesq approximation in 3-D spherical shell at high Rayleigh numbers. For simplicity, we ignored the effects of various complexities expected for the mantle materials, such as viscosity variation, internal heating, and phase transitions. Therefore the parameter is only the basal heating Rayleigh number Ra . Yanagisawa and Yamagishi²⁾ carried out the simulations of the thermal convection in spherical shell for wide range of Ra , and succeeded in calculating the convection at the higher Ra than in the existing studies.

Shown in Figure 1 are the temperature distributions of the convection with $Ra \sim 10^4, 10^6, 10^8$ in the thermally balanced state for three depths. This state means that the total heat flow

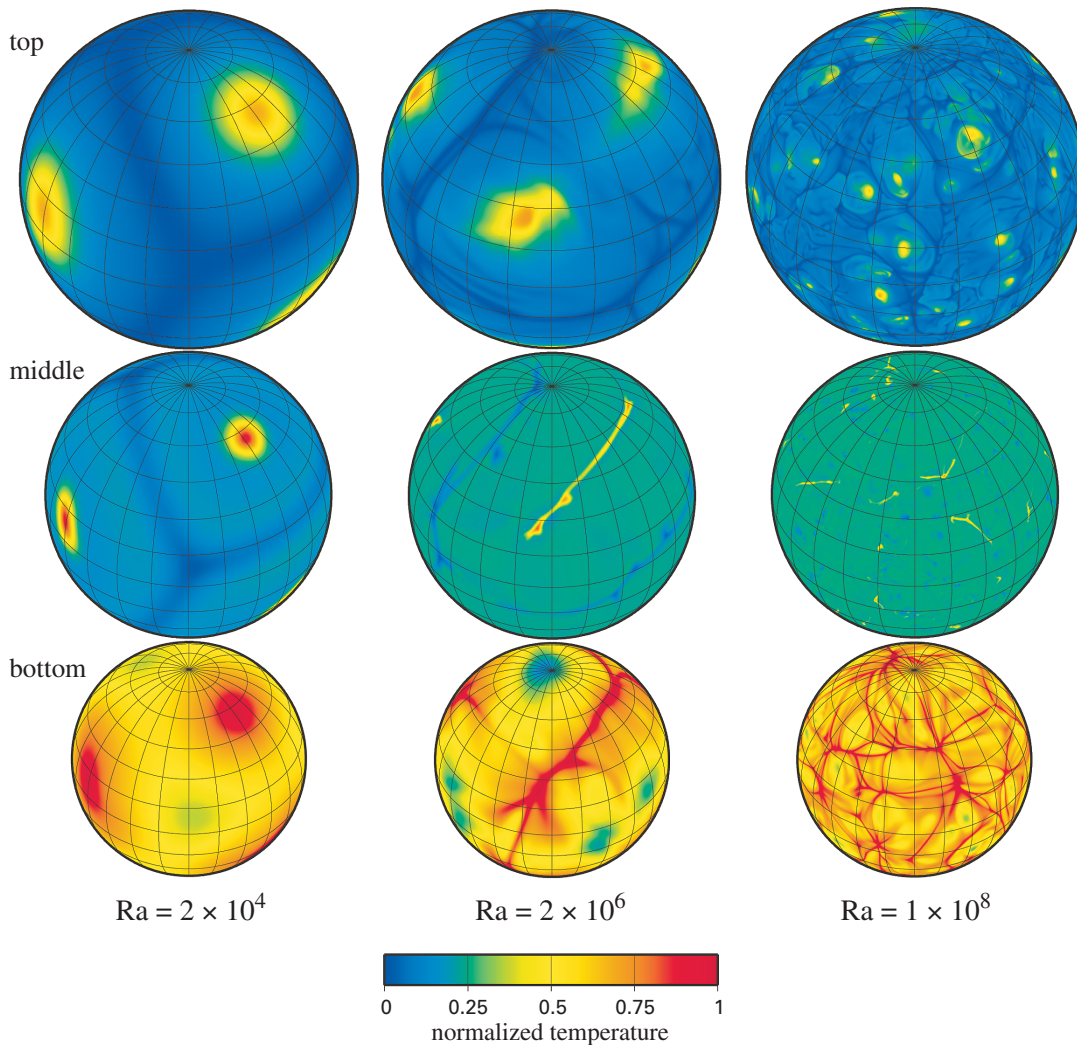


Fig. 1 Simple high Rayleigh number convection. The temperature distributions of the convective shell for $Ra \sim 10^4, 10^6, 10^8$. Ra increases from left to right. The first row is adjacent to the top thermal boundary layer, the second row is the middle depth, and the third row is adjacent to the bottom thermal boundary layer.

from the top is nearly equal to that thorough the bottom. Figure 1 shows that the convective cells become smaller with increasing Ra . In addition, for the lower Ra , the convective cells have almost uniform size, but for the higher Ra , the cells become irregular. All of the convective patterns shown here are characterized as follows; the sheet-shaped downwelling and upwelling flows are generated around the top and the bottom boundaries, respectively, and they concentrate gradually into cylindrical flows in the convective core region. The convection motion for $Ra \sim 10^6, 10^8$ are fluctuating, and the time scale of the fluctuation becomes shorter as Ra increases.

We also calculate the efficiency of the convective heat transport, namely Nusselt number, Nu , which is defined by the ratio of the heat flux of the convective to the conductive state. By compiling the numerical results, we obtain the relationship that Nu is proportional to $Ra^{0.30}$. We further confirm that this relation holds up to $Ra = 10^8$, the highest Ra employed in this study.

3. The effect of the 660 km phase transition on the mantle convection

The endothermic phase transition at 660 km depth of the mantle acts as a barrier for the vertical flow, and its value of Clapeyron-slope controls the global convection pattern. We reported on this problem last year for the range $Ra < 10^7$. This year, we extended Ra range and carried out systematic calculation by varying the value of the Clapeyron-slope at the 660 km depth dP/dT_{660} . The results in the previous section ensure that our simulation code works well up to $Ra = 1 \times 10^8$. The spatial resolution is as fine as about 15 km on the Earth's surface. Figure 2 shows the regime diagram of the convection patterns summarizing the numerical results performed with various values of Ra and dP/dT_{660} . When Ra is 7×10^4 the convection shows a whole layer pattern regardless of the values of dP/dT_{660} employed here. For the cases between $Ra = 7 \times 10^5$ and 1×10^8 , however, the convection style varies with

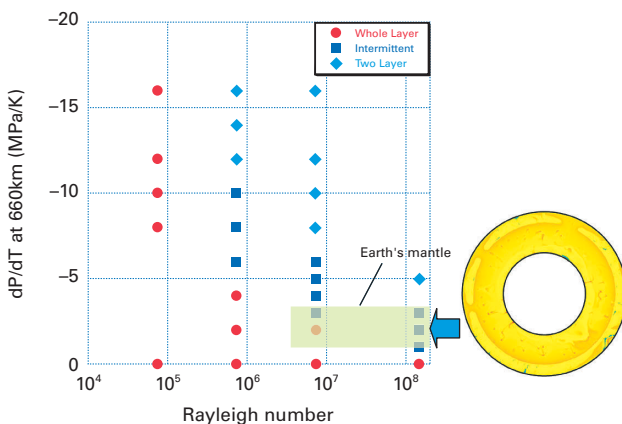


Fig. 2 The effect of endothermic phase transition at 660 km depth of the mantle. Regime diagram of the convection patterns summarizing the numerical simulations for spherical shell performed with various values of Ra and Clapeyron-slope dP/dT_{660} .

dP/dT_{660} ; with the increase of $|dP/dT_{660}|$, the style shifts from the whole layer convection to two-layered one. There exists the intermittent convection region between the whole layer and two layered style. As Ra increases, the intermittent state between the convective regimes appears at smaller $|dP/dT_{660}|$. In other words, the convection tends to be separated at 660 km depth for a large Ra , which is consistent with the previous studies. Figure 2 also shows the ranges of dP/dT_{660} relevant to the Earth, estimated from the high-pressure experiments. Taken together with the estimates of the Ra under the Earth's conditions, the mantle convection of the Earth is most likely to belong to the intermittent regime. This is consistent with the image of the mantle obtained by seismic tomography.

4. Numerical modeling on generation of stagnant slabs

3-D spherical shell model of mantle convection is useful to understand the global flow pattern and long-term evolution. But it has limitations to include many complexities that the real Earth has. Together with the 3-D global model, we are making up 2-D regional models for simulating more realistic subduction process.

We construct models of subducting plates with movable plate boundaries self-consistently integrated into the mantle convection system to investigate interaction of the subducted slab with the mantle transition zone. In these models, we investigate dynamic feedback effects between the slab instability and interaction with the phase transitions. Figure 3 shows two examples of the influence of the freely movable plate boundary. In the case of fixed plate boundary (the top), the 660 km phase transition cannot prevent the slab from penetrating in the lower mantle. The buoyancy of the slab does not act effectively on the 660 km phase transition because a stiff slab is subducted vertically. In the case of freely movable plate (bottom), the slab sinks gradually with a shallow dip angle. In this case, the slab penetration is impeded and a hori-

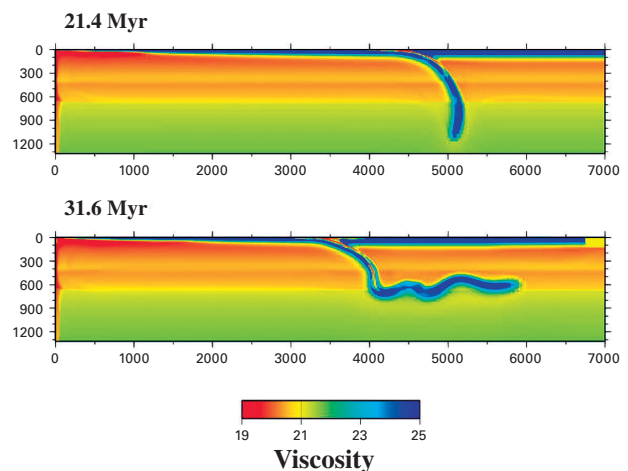


Fig. 3 Regional model for subduction. Snapshots of subduction models with fixed (the top) and freely movable plate boundaries (the bottom). In the latter case, viscosity reduces due to slow grain growth by the phase transition due to the low temperature in the slab.

zontally lying slab is formed at the 660 km phase transition. The behavior of the slab for this case is basically consistent with the structure and evolution around NW Pacific region including the Japanese Islands. We have also examined effects of the slab rheology in the transition zone and temperature- and pressure- dependent thermal expansivity.

5. Numerical modeling of turbulent mixing in volcanic eruption clouds

As the consequence of slab subduction, some amount of molten rock generates at the specific region of the mantle. It gets together to make up magma chambers, and then volcanic activities occur along subduction zones like Japanese Islands. Although there are many complicated processes before a volcanic eruption, here we model the observable surface phenomenon, that is volcanic eruption clouds. Explosive volcanism is one of the most catastrophic phenomena at the boundary of the solid earth and atmosphere. The eruption cloud is the mixture of the volcanic gas, ash and entrained air, and its dynamics are governed by the turbulent mixing. We have developed the Ash77 code which is based on the finite difference method for compressible flow of fluid with high Reynolds number. The details of this code are described in Suzuki et al.³⁾. By virtue of the spatial discretization of third order accuracy, we successfully reproduced the 3-D behavior of eruption clouds including the formation of eruption columns, pyroclastic flows and umbrella clouds (Figure 4). Figure 4 shows that the mass fraction of the ejected material decreases as the eruption cloud rises to the eruption column and radially spreads in the umbrella cloud because of the efficient turbulent mixing.

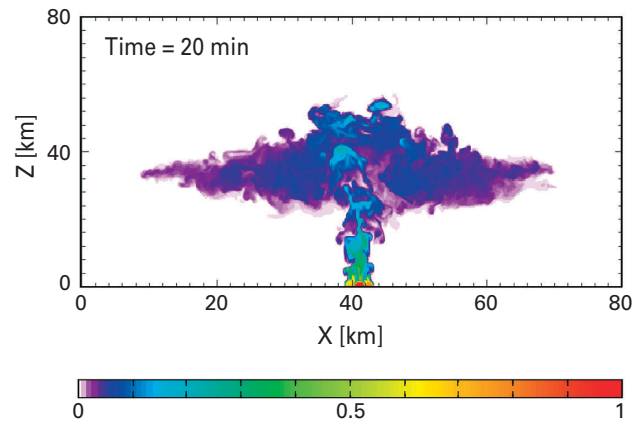


Fig. 4 Modeling of volcanic eruption. Numerical result of umbrella cloud at 20 min from the beginning of eruption. Cross-sectional distribution of the mass fraction of the ejected material are shown in x-z space.

References

- 1) Fukao, Y., S. Widiyantoro, and M. Obayashi, "Stagnant slabs in the upper and lower mantle transition region", *Rev. Geophys.*, vol.39, pp.291–323, 2001.
- 2) Yanagisawa, T., and Y. Yamagishi, "Rayleigh-Benard convection in spherical shell with infinite Prandtl number at high Rayleigh number", *Journal of the Earth Simulator*, vol.4, pp.11–17, 2005.
- 3) Suzuki, Y. J., T. Koyaguchi, M. Ogawa, and I. Hachisu, "A numerical study of turbulent mixing in eruption clouds using a three-dimensional fluid dynamics model", *J. Geophys. Res.*, vol.110, B08201, 2005.

マントル対流と沈み込み過程の数値シミュレーション

プロジェクト責任者

深尾 良夫 海洋研究開発機構 地球内部変動研究センター

著者

深尾 良夫^{*1}, 中久喜伴益^{*2}, 亀山 真典^{*3}, 柳澤 孝寿^{*1}, 山岸 保子^{*1}, 鈴木雄治郎^{*1},
鈴木 厚^{*4}, 木戸 元之^{*5}, 小河 正基^{*6}, 江口 孝雄^{*7}, 岩瀬 康行^{*7}, 中川 貴司^{*8},
多川 道雄^{*2}, 平山 義人^{*7}, Millard F. Coffin^{*9}, John Baumgardner^{*10}, Mark Richards^{*11},
Dave Stegman^{*12}, Stephan Labrosse^{*13}

*1 海洋研究開発機構 地球内部変動研究センター

*2 広島大学大学院 理学研究科

*3 海洋研究開発機構 地球シミュレーターセンター

*4 九州大学 数理学研究院

*5 東北大学 地震・噴火予知研究観測センター

*6 東京大学 大学院総合文化研究科

*7 防衛大学校 応用科学群地球海洋学科

*8 東京大学 大学院理学系研究科

*9 東京大学 海洋研究所

*10 ロスアラモス国立研究所

*11 カリフォルニア大学バークレー校

*12 モナッシュ大学 数理科学研究科

*13 パリ大学 地球物理研究科

地球のマントルは固体の岩石で構成されている。しかし地質学的な時間で見るとマントルは流動していてプレート運動として地表に現れ、プレート境界で地震や火山という現象を引き起こす。更に長い時間スケールでは日本列島のような島弧やヒマラヤのような大山脈を作り出す原因となっている。プレートは海溝より地球内部に沈み込んでいるが、その先はどのようになっているのだろうか。地震波トモグラフィーによりマントル中での沈み込んだプレートの様子が描き出されている。それによれば沈み込み帯からプレートの延長と考えられる構造(スラブ)がマントル遷移層の深さまで到達し、地球上の多くの場所ではそのまま遷移層に横たわっている。これらはスタグナントスラブと呼ばれる。日本列島も含めた東アジア地域はスタグナントスラブの上方に位置している。そのため、どのようにしてスタグナントスラブが形成されてきたのか、さらに将来このような構造はどうなっていくのか、という問題は我々が生存している場の理解にとって重要である。本課題では今年度、3通りのモデリングでこのようなマントルの挙動とプレート沈み込みに伴う火山現象の理解を進めた。

- 1) 3次元球殻による全球モデリング: 計算格子の地表での水平スケールを15kmにまで細かくすることに成功し、マントルのような高粘性流体の計算としては世界最高のレイリー数(下部加熱)に到達した。これにより、細かい複雑性を考慮せずに全球を同時に扱うという観点では、地球史の大部分に適用できるレイリー数領域での計算が可能となった。これに基づき、マントル遷移層で重要な役割を果たす吸熱相転移が対流パターンに与える影響を調査し、スタグナントスラブが存在し得る条件を確定した。
- 2) 2次元矩形領域での沈み込みモデリング: 大規模粘性変化、大陸の存在、プレート構造と複雑レオロジー、など全球モデルでは扱いが困難な効果を考慮した領域モデルを作り上げ、沈み込んだスラブが時間の経過とともに自発的に横たわっていく過程の再現に成功した。
- 3) 3次元での火山噴煙モデリング: 沈み込み帯には爆発的な噴火を起こす火山が存在する。高レイノルズ数で圧縮性流体を扱うコードの開発を進め、火口からの高温の噴出物が周囲の大気を取り込んで上昇し、傘型の噴煙を形成する過程を再現することに成功した。

キーワード: マントル対流, プレート運動, 沈み込み帯, スタグナントスラブ, 火山噴火